Demonstration of coupling to symmetric and antisymmetric cladding modes in arc-induced long-period fiber gratings

Gaspar Rego[*], Oleg V. Ivanov, and P.V.S. Marques[**]

Unidade de Optoelectrónica e Sistemas Electrónicos, INESC Porto, R. Campo Alegre 687, 4169-007 Porto, Portugal
[*] also with Escola Superior de Tecnologia e Gestão-IPVC, 4900–348 Viana do Castelo, Portugal
[**] also with Departmento de Física, Faculdade de Ciências da Universidade do Porto, 4169-007 Porto, Portugal
gmrego@fc.up.pt, olegivvit@yandex.ru

Abstract: The symmetry of cladding modes excited in microbend and arc-induced long-period fiber gratings is investigated. An optimization technique is developed to determine the fiber parameters and to associate grating resonances with cladding modes of a particular symmetry. Using this optimization procedure, we show that the gratings induced in a standard fiber by arc discharges and microbends couple light to the antisymmetric cladding modes. In the case of a boron-germanium codoped fiber, the cladding modes excited by arc-induced gratings are found to be symmetric. Measurements of the near-field intensity distribution of cladding modes confirm the mode symmetry ascertained by the optimization technique.

OCIS codes: (060.2340) Fiber optics components, (050.2770) Gratings

References and Links

1. O. V. Ivanov, S. A. Nikitov, and Yu. V. Gulyaev, "Cladding modes of optical fibers: properties and applications," Physics-Uspekhi **49**, 175-202 (2006).
2. S. W. James and R. P. Tatam, "Optical fibre long-period grating sensors: characteristics and application," Meas. Sci. Technol. **14**, R49–R61 (2003).
3. G. Rego, O. Okhotnikov, E. Dianov, and V. Sulimov, "High-temperature stability of long-period fiber gratings produced using an electric arc," J. Lightwave Technol. **19**, 1574-1579 (2001).
4. F. Durr, G. Rego, P. V. S. Marques, S. L. Semjonov, E. Dianov, H. G. Limberger, and R. P. Salathe, "Stress profiling of arc-induced long period fiber gratings," J. Lightwave Technol. **23**, 3947-3953 (2005).
5. G. Rego, J. R. A. Fernandes, J. L. Santos, H. M. Salgado, and P. V. S. Marques, "New technique to mechanically induce long-period fibre gratings," Opt. Commun. **220**, 111–118 (2003).
6. S. Kim, Y. Jeong, S. Kim, J. Kwon, N. Park, and B. Lee, "Control of the characteristics of a long-period grating by cladding etching," Appl. Opt. **39**, 2038–2042 (2000).
7. J. W. Fleming, "Dispersion in GeO_2-SiO_2 glasses," Appl. Opt. **23**, 4486–4493 (1984).
8. G. Rego, L. Santos, B. Schroder, P. Marques, J. L. Santos, and H. M. Salgado, "In situ temperature measurement of an optical fiber submitted to electric arc discharges," IEEE Photon. Technol. Lett. **16**, 2111–2113 (2004).
9. G. Rego, J. L. Santos, and H. M. Salgado, "Polarization dependent loss of arc-induced long-period fibre gratings," Opt. Commun. **262**, 152–156 (2006).

1. Introduction

A long-period fiber grating (LPFG) is a fiber structure with a periodic perturbation of its refractive index (RI), which couples the core mode and copropagating cladding modes. Due to the fact that the grating period is of the order of hundreds of micrometers, the fabrication of LPFGs may be quite simple and several techniques have been demonstrated [1,2]. Historically, the first LPFGs were produced by microbending. The perturbation induced in microbend gratings is antisymmetric. The photoinduced LPFGs are created by exposure of the fiber to UV radiation and have a symmetric modulation of the RI. Another type of LPFG is based on a periodical heating of the fiber by exposure to arc discharges [3].

While the mechanism of formation of microbend and photoinduced LPFGs is well understood, the mechanism of formation of arc-induced LPFGs is still under dispute [4].

#70368 - $15.00 USD Received 26 April 2006; revised 7 July 2006; accepted 31 July 2006

Several mechanisms were presumed, but no predominant mechanism was found, which indicates that more than one may contribute to the grating formation. It is also unclear if symmetric or antisymmetric perturbation is induced by the arc discharge and, correspondingly, if symmetric or antisymmetric cladding modes are involved in the coupling in these gratings. Therefore, the investigation of mode symmetry is important for the determination of the mechanism of formation of arc-induced LPFGs.

In principle, the symmetry of cladding modes can be determined by comparison of the experimental spectrum of an LPFG and the spectrum obtained by simulation for modes of a particular symmetry. In practice, however, such a comparison is impossible because usually the accuracy of fiber parameters given in the specification sheet is insufficient for accurate reproduction of LPFG spectra and for discrimination between symmetric and antisymmetric modes. In addition, the fiber parameters are modified during the grating writing process.

In this paper, we attempt to reveal if symmetric or antisymmetric cladding modes are excited in the arc-induced LPFGs and get some understanding about the mechanism of grating formation. For this, we employ an optimization technique to fit experimental and theoretical dependences of resonance positions on the grating period, which allows us to determine the fiber parameters. We apply those parameters to simulate the gratings transmission spectra and compare with the experimental ones. The results obtained by the optimization technique are supported by measurements of the near-field intensity distributions of the cladding modes.

2. Experimental

Three types of gratings are studied in this work: microbend LPFGs in Corning SMF-28 fiber, arc-induced LPFGs in Corning SMF-28 fiber, and arc-induced LPFGs in Fibercore PS1250/1500 fiber. Microbend LPFGs were mechanically induced by winding a nylon string around a brass tube with a fiber pressed against the grooves [5]. The evolution of the gratings spectra was monitored using a white light source and an optical spectrum analyzer. The spectrum of each grating contains several resonances, whose positions are shown in Fig. 1(a) as a function of the grating period (squares). Figure 2(a) shows the spectrum of a 600 μm grating (solid curve).

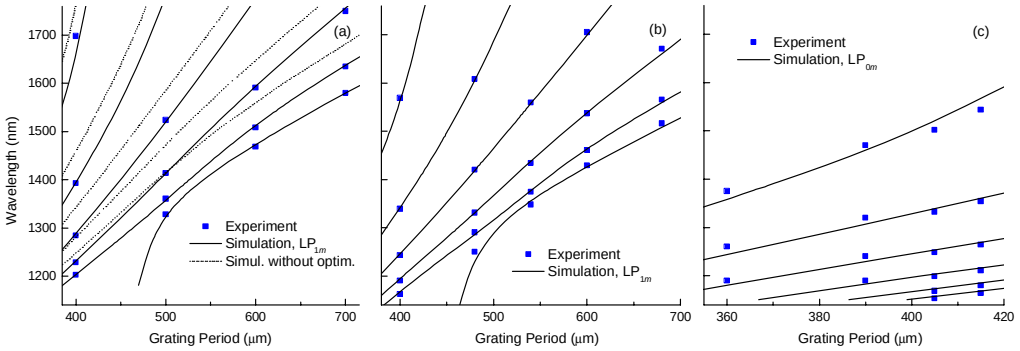

Fig. 1. Resonance wavelengths of cladding modes excited by (a) microbend LPFG in SMF-28 fiber, (b) arc-induced LPFG in SMF-28 fiber, and (c) arc-induced LPFG in PS1250/1500 fiber versus period. The squares are experimental data; the curves are simulation results.

To fabricate arc-induced LPFGs an uncoated fiber was fixed between the electrodes of a fusion splicing machine. One end of the fiber was clamped in a fiber holder on top of a motorized translation stage whose displacement was controlled with a precision of 0.1 μm. At the other end a weight was attached to keep the fiber under a constant tension (1–40 g). Since the mechanism of grating formation may be different for different fibers, we wrote LPFGs in two types of fibers: Corning SMF-28 fiber with a 8.2 μm diameter germanium-doped core and a RI difference Δn = 0.0052 and Fibercore PS1250/1500 fiber having a core codoped with

#70368 - $15.00 USD Received 26 April 2006; revised 7 July 2006; accepted 31 July 2006

about 10% of germania and about 20% of boron oxide. There is no definite data on the core size of the latter fiber, but different sources indicate that the core radius is in the region of 3.5–4.5 μm.

A series of gratings with various periods was written in each of the two fibers. The positions of their cladding mode resonances are shown by squares in Figs. 1(b) and 1(c). The spectra for gratings with periods of 540 μm (SMF) and 415 μm (PS) are presented by solid curves in Figs. 2(b) and 2(c), respectively. As it can be seen in Fig. 1, the resonance wavelengths of all gratings increase with an increase in the period. For some gratings such an increase from one period to another may be so large that it becomes difficult to associate a resonance of a particular cladding mode in the spectrum of one grating with the resonance of the same mode in the spectrum of the other grating (with a different period). In this case, to connect correctly the data points it is necessary to analyze thoroughly the whole dependence of all resonance wavelengths on the grating period.

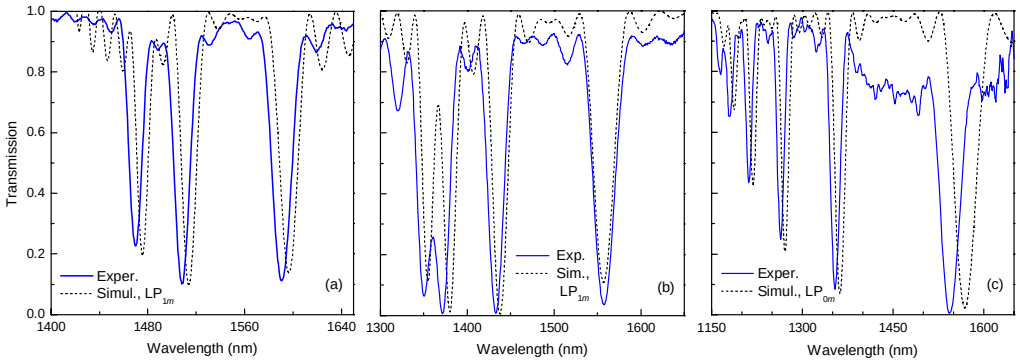

Fig. 2. Spectra of (a) a 600-μm LPFG mechanically induced in SMF-28 fiber, (b) a 540-μm LPFG arc-induced in SMF-28 fiber, and (c) a 415-μm LPFG arc-induced in PS1250/1500 fiber. The solid curves are experimental data; the dashed curves are simulation results.

3. Optimization procedure

Normally, the analysis of transmission through LPFGs requires a solution to the problem of finding correspondence between experimental and theoretical spectra. The difficulty of this problem is that very small deviations of fiber parameters from the nominal specifications result in significant changes in the transmission spectra. For example, the shift of resonance wavelength of a standard LPFG as a result of a 2% change in the difference between the core and cladding RIs (from Δn = 0.0054 to 0.0055) is of the order of 30 nm. Moreover, some parameters such as core radius or dopant concentration are frequently unknown or unspecified. Such fiber parameters as refractive index, core and cladding radii can be changed as a result of grating formation in the fiber: refractive index is changed in the photoinduced gratings and, in addition, fiber dimensions are changed in the arc-induced gratings.

Therefore, it becomes impossible to directly compare experimental data with theoretical calculations. In the case of arc-induced gratings, it is also not clear what is the kind of modes that are excited by the grating. Furthermore, it is not always possible to attribute a particular mode number to a resonance in the spectrum due to the presence of small amplitude resonances that are indistinguishable from the background noise. This is especially important for modes with low radial mode numbers whose resonances are in the short wavelength range and close to the cutoff wavelength.

In order to carry out the comparison indicated above, to ascertain the symmetry of modes (i.e., to determine their azimuthal mode number), and to find the radial mode numbers, we developed a procedure for optimization of the fiber parameters, which fits theoretical resonance positions to the experimental ones. The optimization procedure was constructed as

#70368 - $15.00 USD Received 26 April 2006; revised 7 July 2006; accepted 31 July 2006

follows. The phase matching condition for the core mode and one of the cladding modes coupled by an LPFG is written in the form of

$$\beta^{(\mathrm{co})} - \beta_i^{(\mathrm{cl})} = 2\pi/\Lambda\,, \tag{1}$$

where $\beta^{(\mathrm{co})}$ and $\beta_i^{(\mathrm{cl})}$ are the propagation constants of the core mode and of the *i*-th cladding mode, and Λ is the grating period. From the experimental transmission spectrum of an LPFG, it is possible to find the resonance wavelengths of a series of cladding modes. The same resonance wavelengths can be calculated for a given set of fiber parameters and compared with the experimental ones. However, the calculation of resonance wavelengths requires considerable computational work; therefore, we use the following quantities to characterize the discrepancy between the propagation constants of the experimental and theoretical modes:

$$f_{ijk}(\mathbf{u}) = \beta^{(\mathrm{co})}(\lambda_{ijk}, \mathbf{v}_k, \mathbf{u}) - \beta_i^{(\mathrm{cl})}(\lambda_{ijk}, \mathbf{v}_k, \mathbf{u}) - 2\pi/\Lambda_j\,, \tag{2}$$

where the value of period is experimental and the propagation constants are found by calculation at wavelength λ_{ijk} for a particular grating period Λ_j, a set of fixed fiber parameters is defined by the vector $\mathbf{v}_k$, and variable fiber parameters are defined by the vector $\mathbf{u}$. The vector $\mathbf{v}_k$ is used here for the case of spectra measured with different fiber parameters, for example, in the experiment where the resonance position was measured as a function of the cladding radius reduced by etching [6]. The overall proximity of the presumed fiber structure to the real structure is described by the optimization function, which takes into account the deviations for various resonances and various fiber and grating parameters:

$$F(\mathbf{u}) = \sum_{i,j,k} f_{ijk}^2(\mathbf{u})\,. \tag{3}$$

Here, the function $F(\mathbf{u})$ is obtained by summation over resonances (*i*), grating periods (*j*), and sets of fiber parameters (*k*). Ideally, in the case of complete coincidence of the presupposed $\mathbf{u}$ with the real $\mathbf{u}$, $F = 0$. However, there are always measurement errors, which make the absolute minimum of $F = 0$ unachievable in practice.

4. Analysis

In order to determine the type of modes excited by arc-induced gratings we need to search for such fiber parameters, type of modes, and mode numbers for which the optimization function attains its minimum. In the present work, we optimize two fiber parameters—the core radius and the dopant concentration. We assume the fibers to be step-index with uniform refractive indices in the core and the cladding. The RIs of cladding and of germanium-doped core are calculated using Fleming's formula [7].

We suppose that modes of two types can be induced in the gratings under study—symmetric (LP_{0i}) and antisymmetric (LP_{1i})—since there is no reason for the appearance of higher order perturbations in the fiber. Even if such perturbations exist, their amplitude should be significantly smaller than the amplitudes of symmetric and antisymmetric perturbations. We also assume that small amplitude resonances of low order modes may be present in the short-wavelength side of the spectra. If these resonances exist they are not revealed and are not given in Fig. 1. Therefore we introduce the parameter n_{mis} that is equal to the number of resonances missed; i.e., the resonances with $i = 1,\ldots, n_{\mathrm{mis}}$ are missed and the resonances with $i = n_{\mathrm{mis}} + 1,\ldots$ are not. At the same time, we assume that there are no missed resonances between the resonances revealed. So, there is a shift in the numeration of cladding modes and we should replace $\beta_i^{(\mathrm{cl})}(\lambda_{ijk}, \mathbf{v}_k, \mathbf{u})$ in Eq. 2 by $\beta_{i+n_{\mathrm{mis}}}^{(\mathrm{cl})}(\lambda_{ijk}, \mathbf{v}_k, \mathbf{u})$.

In order to test and verify that the optimization technique allows us to determine the type of modes excited by LPFGs, we first analyzed microbend gratings, whose modulation, as is well known, is antisymmetric and, correspondingly, the core mode is coupled to antisymmetric cladding modes LP_{1i}.

The results of application of the optimization technique to the microbend LPFGs are shown in the upper part of Table 1. We searched over the two parameters n_{mis} and the type of symmetry. The optimization function has a minimum value of $F = 0.5 \cdot 10^4\ \mu\mathrm{m}^2$ for $n_{\mathrm{mis}} = 0$ and

#70368 - $15.00 USD Received 26 April 2006; revised 7 July 2006; accepted 31 July 2006

for the antisymmetric type of modes. The second minimum value is $F = 16.87 \cdot 10^4$ μm^2 and is much greater than the first minimum value of F. This strongly indicates that the first minimum corresponds to the real situation but not the second. Thus, we established that the optimization technique proposed confirms that the antisymmetric modes are excited in the microbend gratings. We also obtained parameters of the fiber core: r_{co} = 4.33 μm and $C(GeO_2) = 3.31\%$.

Table 1. Results of optimization for the three gratings

Grating, fiber	n_{mis}	Symmetry	F×10^4 (μm^2)	r_{co} (μm)	GeO_2 (%)	B_2O_3 (%)
microbend, SMF-28	0	sym	16.87	4.35	3.20	0
	0	**antisym**	**0.50**	**4.33**	**3.31**	**0**
	1	sym	114.26	2.99	4.11	0
	1	antisym	46.47	3.73	3.42	0
arc-induced, SMF-28	0	sym	19.73	4.06	3.22	0
	0	**antisym**	**0.55**	**4.22**	**3.23**	**0**
	1	sym	111.83	2.56	4.52	0
	1	antisym	57.31	3.23	3.64	0
arc-induced, PS1250/1500	**0**	**sym**	**2.94**	**2.72**	**10**	**20.71**
	0	antisym	6.41	3.09	10	22.32
	1	sym	6.02	1.62	10	10.60
	1	antisym	1.93	1.66	10	11.26

For the parameters found, we calculated the positions of resonance wavelengths versus period. They are shown by solid curves in Fig. 1(a). It is seen that the simulation curves fit very well the experimental data. For comparison, we give results of simulation for the LP_{1m} modes carried out for unoptimized fiber parameters (dotted curves in Fig. 1(a)). These simulation curves are far from experimental points and cannot be used for the determination of mode symmetry. We also calculated the spectrum of one microbend LPFG using Apollo Photonics v2.2a software. It is given in Fig. 2(a) by the dashed curve and is close to the experimental spectrum.

Next we used the optimization for investigating the symmetry of cladding modes excited in the LPFGs induced by arc discharges in the SMF-28 fiber. The second part of Table 1 shows the minima of the optimization function found for various combinations of n_{mis} and mode symmetries. As is seen from Table 1, the best correspondence with the experimental data takes place for $n_{mis} = 0$ and antisymmetric type of modes. This allows us to conclude that for the arc-induced gratings the core mode is coupled to the LP_{1i} cladding modes. Figure 1(b) shows a simulation of the dependences of resonance positions (solid curves) as a function of the period for gratings arc-induced in the SMF-28 fiber. The simulated spectrum of one grating with a period of 540 μm is depicted in Fig. 2(b) (dashed curve).

For the same period, the resonance wavelengths of arc-induced gratings are shorter than those of microbend LPFGs. The difference obtained may be due to stress relaxation/viscoelasticity produced by the arc discharge. The fiber reaches a temperature of about 1320 ºC during the arc discharge and, therefore, high temperature partially anneals its intrinsic stresses [8]. This may result in modification of the fiber RI profile.

An analogous optimization procedure was carried out for the PS1250/1500 fiber. In contrast to the standard fiber, the core of this fiber has higher concentration of germanium and, in addition, is doped with boron. Due to this fact, it becomes more difficult to evaluate the RI of the core for various dopant concentrations at different wavelengths. To calculate the RI of the core we used the RI of silica doped with 10% of germania, and after that a correction given by $\Delta n = -\alpha C(B_2O_3)$ was introduced, which was independent on the wavelength (here $\alpha = 0.04$ and $C(B_2O_3)$ is the concentration of boron oxide).

#70368 - $15.00 USD Received 26 April 2006; revised 7 July 2006; accepted 31 July 2006

The results of the optimization for the B/Ge fiber are presented in the lower part of Table 1. The difference between the values of the optimization function is not as large as in the case of the standard fiber probably due to imperfect method of calculating the RI of silica codoped with germania and boron. The minimum of the optimization function is for $n_{mis} = 1$ and antisymmetric modes; however, the optimal core radius (1.66 μm) and boron oxide concentration (11.26%) are much smaller than expected. Therefore, we suppose that this minimum is irrelevant and we neglect it. The second minimum occurs for $n_{mis} = 0$ and symmetric type of modes. It follows from here that in the PS1250/1500 fiber, in contrast to the SMF-28 fiber, the cladding modes are symmetric. This indicates different mechanism of grating formation in these two fibers.

Thus, it was demonstrated that both types of perturbation can be induced by arc discharges. We can point to three possible origins of antisymmetric perturbations in the arc-induced LPFGs: asymmetry of the arc and temperature distribution with respect to the fiber center, asymmetry of the fiber, and spontaneous asymmetry. We suppose that the main reason is the first one, which is due to misalignment of the fiber between the electrodes during the gratings fabrication or asymmetry of the arc itself. To verify this hypothesis we are going to study the effect of fiber shift between the electrodes and to publish the result elsewhere. Since the perturbation arc-induced in the standard fiber is asymmetric, properties of the corresponding LPFG should be polarization dependent [9].

In order to confirm the symmetry of the perturbations in the fiber, the near fields of several cladding modes excited by arc-induced gratings were measured. The fiber was cleaved just after the grating and the near field of the radiation emerging from the fiber-end was detected by an infrared camera, while the tunable laser (HQ4321A) used as a source scanned the wavelength around a particular grating resonance (positioned between 1520 and 1620 nm). Figure 3 shows the near fields of two resonances observed at 1551 nm and 1543 nm which correspond to the grating spectra shown in Figs. 2(b) and 2(c), respectively. The intensity distribution presented in Fig. 3(a) shows that the arc-induced LPFGs in the standard fiber couple to antisymmetric LP_{1i} cladding modes, while the distribution in Fig. 3(b) shows that the same gratings in B/Ge codoped fiber couple to symmetric LP_{0i} cladding modes.

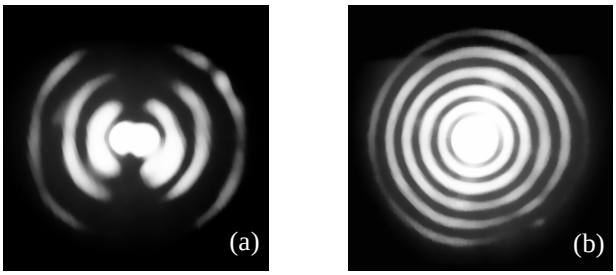

Fig. 3. Near-field intensity distributions of (a) LP_{14} cladding mode of a 540-μm LPFG arc-induced in the SMF-28 fiber and (b) LP_{07} cladding mode of a 415-μm LPFG arc-induced in the PS1250/1500 fiber.

5. Conclusion

An optimization procedure was developed in order to refine the values of fiber parameters by fitting simulation to experimental data on resonance wavelengths of LPFGs. This procedure was used to associate the grating resonances observed in the spectra to particular cladding modes. The symmetry of cladding modes excited by microbend and arc-induced gratings in the standard fiber and boron-germanium codoped fiber was revealed: microbend and arc-induced LPFGs in the standard fiber couple the core mode to the antisymmetric cladding modes, while arc-induced LPFGs in boron-germanium codoped fiber excite symmetric cladding modes. This was also confirmed by measurements of the near-field patterns of some of those cladding modes.

#70368 - $15.00 USD Received 26 April 2006; revised 7 July 2006; accepted 31 July 2006